NASA TECHNICAL NOTE

NASA TN D-4883

NASA TN D-4883

NASA TN D-4883
pt. 1
c. 1

TECH LIBRARY KAFB, NM
0131508

LOAN COPY: RETURN
AFWL (WLIL-2)
KIRTLAND AFB, N M.

EXPERIMENTS ON THE STABILITY OF WATER LUBRICATED HERRINGBONE-GROOVE JOURNAL BEARINGS

I - Theoretical Considerations and Clearance Effects

by Fredrick T. Schuller, David P. Fleming, and William J. Anderson

Lewis Research Center
Cleveland, Ohio

NATIONAL AERONAUTICS AND SPACE ADMINISTRATION • WASHINGTON, D. C. • NOVEMBER 1968

NASA TN D-4883

TECH LIBRARY KAFB, NM
0131508

EXPERIMENTS ON THE STABILITY OF WATER LUBRICATED HERRINGBONE-GROOVE JOURNAL BEARINGS I - THEORETICAL CONSIDERATIONS AND CLEARANCE EFFECTS

By Fredrick T. Schuller, David P. Fleming, and William J. Anderson

Lewis Research Center
Cleveland, Ohio

NATIONAL AERONAUTICS AND SPACE ADMINISTRATION

For sale by the Clearinghouse for Federal Scientific and Technical Information
Springfield, Virginia 22151 – CFSTI price $3.00

ABSTRACT

Hydrodynamic journal bearing stability tests were conducted with three different herringbone journal configurations. The bearings had a 1.5-inch (3.8-cm) diameter and were tested in water at 80° F (300 K) at speeds to 12 000 rpm, with unit loads to 36.9 psi (25.4×10^4 N/m^2). The stability of herringbone-groove journal bearings was far superior to that of a 100° partial-arc bearing, especially at zero load. No significant differences in the zero load threshold of stability were observed among the three different configurations of herringbone journal bearings tested. Theoretical analysis for herringbone-groove journal bearings predicts a larger range of stable operation than was observed experimentally.

EXPERIMENTS ON THE STABILITY OF WATER LUBRICATED HERRINGBONE-GROOVE JOURNAL BEARINGS I - THEORETICAL CONSIDERATIONS AND CLEARANCE EFFECTS

by Fredrick T. Schuller, David P. Fleming, and William J. Anderson

Lewis Research Center

SUMMARY

A series of stability tests was conducted with 1.5-inch (3.8-cm) diameter, 1.5-inch (3.8-cm) long hydrodynamic journal bearings in water at 80° F (300 K) at speeds to 12 000 rpm, with unit loads to 36.9 psi (25.4×10^4 N/m^2). Plain bearings were run at various clearances with three different journals: (1) a partially grooved herringbone journal having 20 groove-ridge pairs, (2) a fully grooved herringbone journal having 20 groove-ridge pairs, and (3) a partially grooved herringbone journal having 40 groove-ridge pairs. The stability of herringbone-groove journal bearings was far superior to that of a 100° partial-arc bearing, especially at zero load. No significant differences in the zero load threshold of stability were observed among the three different configurations of herringbone journal bearings tested. Theoretical analysis, for herringbone-groove journal bearings, predicts a larger range of stable operation than was observed experimentally.

INTRODUCTION

Power-generation systems for space vehicles must incorporate components that are light in weight, possess high reliability, and are of minimum complexity. These requirements apply to each component including the bearings that support any rotating members. The bearing lubrication system can be considerably simplified if the working fluid is used as the bearing lubricant. For the higher power levels (30 to 1000 kW), turbogenerators employing liquid metals as the working fluid are receiving consideration (ref. 1). Hence, if process fluid lubrication is to be used, bearings capable of operating satisfactorily in liquid metals must be developed.

For operation in liquid metals, fluid film bearings have been selected over rolling-element bearings because the former bearing type maintains a full fluid film more easily. This film eliminates or minimizes the rubbing contact problem that is usually present in rolling-element bearings. The most important disadvantage of fluid film bearings is their tendency to exhibit self-excited instability under the light or zero-load conditions that will exist in a space vehicle in a zero-gravity environment. Instability here refers to self-excited fractional frequency whirl, or the tendency of the journal center to orbit the bearing center at an angular velocity about half that of the journal around its own center.

The tilting pad bearing configuration has excellent stability characteristics in sodium (ref. 2). However, it is complex because it is composed of several integral parts. It also is subject to pivot fretting. A journal bearing of fixed geometry that exhibited good stability characteristics when lubricated with air and fair stability when lubricated with sodium is the herringbone-groove bearing (refs. 2 to 4). Because most of the theoretical and experimental work on herringbone-groove bearings has dealt with compressible lubricants (refs. 3 to 5), there is little information available dealing with incompressible lubricants. The experimental data reported herein were compared with theoretical data for incompressible lubricants.

The objectives of this study were (1) to determine the stability characteristics of three water-lubricated herringbone-groove journal bearing configurations with various clearances and (2) to compare experimental stability data for herringbone-groove bearings with analytical predictions. Water was used as the lubricant rather than sodium. This simulation is valid because the viscosity and density of water at 150° F (339 K) closely approximate those of sodium at 400° F (478 K). Stability curves of two bearings having similar geometric configurations and clearances, one run in sodium and the other in water, confirm this contention.

The 1.5-inch (3.8-cm) diameter by 1.5-inch (3.8-cm) long bearings were submerged in water at an average temperature of 80° F (300 K) and operated hydrodynamically at radial loads from 0 to 36.9 psi (25.4×10^4 N/m^2) and journal speeds to 12 000 rpm.

SYMBOLS

a_g	width of helical groove, in.; cm
a_r	width of helical ridge, in.; cm
C	bearing radial clearance, in.; cm
C_1, C_3, C_5, C_6, CP	dimensionless coefficients

D	bearing diameter, in.; cm
e	bearing eccentricity, in.; cm
F_r	restoring force component
F_w	whirl-producing force component
g	gravitational constant, in./sec^2; m/sec^2
H	groove clearance to ridge clearance ratio, h_g/C
h_g	groove clearance $(C + \delta)$, in.; cm
L	bearing length, in.; cm
L_1	length of grooved portion of bearing, in.; cm
M	rotor mass per bearing, W_r/g, (lb)(sec^2)/in.; (kg)(sec^2)/m
$\overline{M}$	dimensionless mass parameter, $MP_a(C/R)^5/(2\mu^2 L)$
M_c	critical mass
$\overline{M}_{cr}$	dimensionless mass parameter $\sqrt{MCW}\,(R/C)^2/(\mu DL)$
N'	journal speed, rps
N_s	whirl onset speed, rpm
N_T	critical transitional journal speed from laminar to turbulent regime, $41.1\,\nu\sqrt{D/2C}/\pi DC$, rps
n	number of grooves
P	film pressure, psi; N/m^2
P_a	atmosphere pressure, psia; N/m^{2}abs
R	journal radius, in.; cm
S	Sommerfeld number, $(\mu N'DL/W)(C/R)^2$
W	applied load, lb; N
W_r	total weight of rotor, lb; N
x	dimensionless axial coordinate z/L
z	axial coordinate, in.; cm
α	ratio of groove width to width of groove and ridge, $a_g/(a_g + a_r)$
β	helix angle, deg
Γ	dimensionless speed parameter, $6\mu\omega(R/C)^2/P_a$
δ	groove depth, in.; cm

ϵ eccentricity ratio, e/c

θ* angular coordinate, rad

μ absolute viscosity, (lb)(sec)/in.^{2}; (N)(sec)/m^2

ν kinematic viscosity, in.^{2}/sec; m^2/sec

ρ lubricant mass density, (lb)(sec^2)/in.^{4}; kg/m^3

φ attitude angle

ω journal angular speed, rad/sec

ω_w whirl frequency, rad/sec

Subscripts:

c neutral stability condition

0 concentric

1 small eccentricity

TEST BEARINGS

Design

Herringbone-grooved journal bearings of three configurations were tested hydrodynamically with the test bearings fully immersed in water. Journals having 20 and 40 partial grooves and 20 full grooves (fig. 1) were evaluated. Shaft rotation was such as to cause inward pumping of the lubricant. The grooves extended beyond the bearing sleeves at each end to ensure an adequate lubricant supply. The partially grooved journals had a circumferential land centrally located along the length of the bearing. The

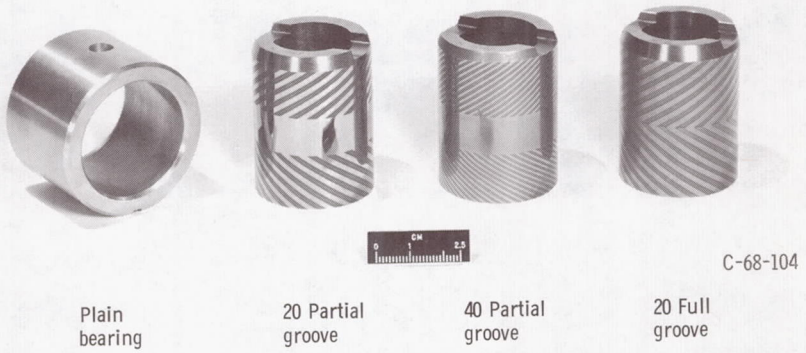

Figure 1. - Herringbone-groove journal configurations.

width of the circumferential land was one-third the length of the bearing (fig. 2). The fully grooved journal had herringbone grooves that met midway along the axial length of the bearing. Surface profile traces were made of each journal outside diameter to obtain the average groove depths listed in table I.

The herringbone journal helix angle and groove to ridge width ratio (table I) were set at those values that yield a maximum radial force at a compressibility number of zero for a compressible lubricant (ref. 5). This approximates the conditions existing with an incompressible lubricant. The analysis of reference 5 assumes an infinite number of

TABLE I. - HERRINGBONE GROOVE GEOMETRIES

Journal	Groove depth, δ		Number of grooves, n	Helix angle, β, deg	Groove width, a_g		Ridge width, a_r		Groove type
	in.	μm			in.	cm	in.	cm	
K-14	0.0014	36	20	33	0.062	0.157	0.062	0.157	Partial
K-15	.0017	43	40	33	.032	.081	.032	.081	Partial
K-6	.0017	43	20	33	.062	.157	.062	.157	Full

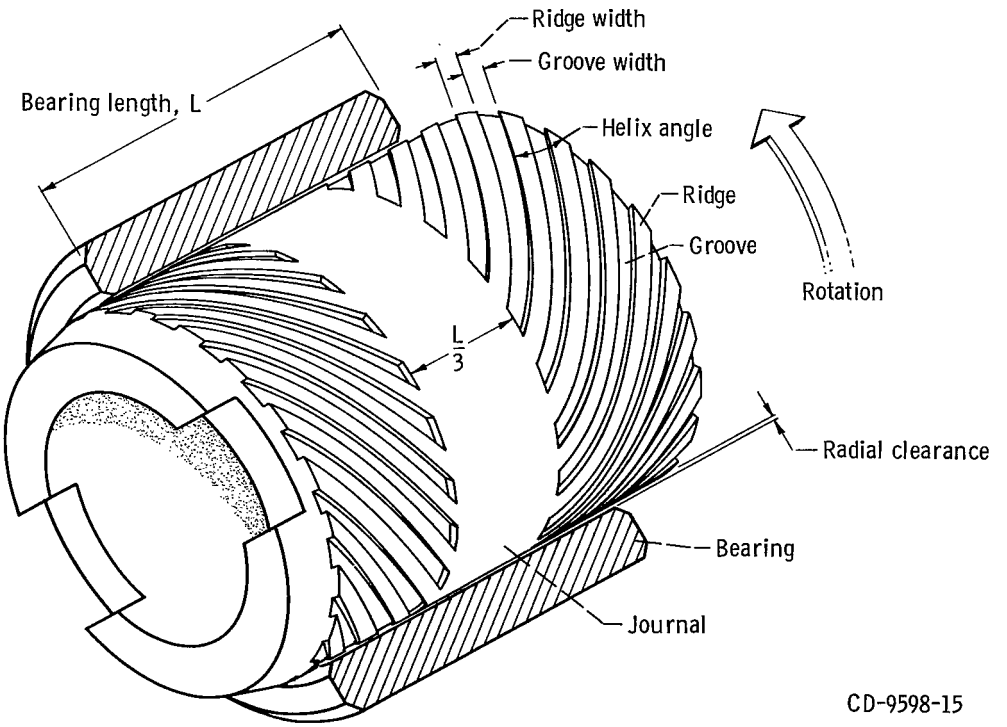

Figure 2. - Partially grooved herringbone journal bearing assembly.

grooves. Because of manufacturing difficulties the maximum number of grooves was set at 40. To study the effect of the number of grooves on bearing stability a 20-groove journal was also incorporated in the tests.

The diameter and length of the bearings in all cases were nominally 1.5 inches (3.8 cm). The journal outside diameter and bearing inside diameter were machined to a 4- to 8-microinch (0.1- to 0.2-μm) rms finish.

APPARATUS

Bearing Test Apparatus

A section of the test vessel and the radial loading system is shown in figure 3. The test bearing was mounted in a housing in the test vessel, and the mating journal was mounted and keyed to the bottom end of the shaft. The shaft was positioned vertically so that gravity forces would not act on the journal. A 15-horsepower (11-kW) direct-current motor powered the shaft through a 7.5 to 1 ratio gearbox. The test vessel was located immediately below the main support bearing housing and floated between upper and lower gas bearings. Two semicircular wheels connected by a cable belt comprised the radial loading system (fig. 3(b)). Radial load was applied by an air cylinder between the two semicircular wheels, one of which pivoted on a knife edge. Bearing torque was measured by a force transducer.

The test shaft was mounted on two support ball bearings that were preloaded to about 200 pounds (890 N) by a wave spring. This preload was necessary to ensure a minimum amount of shaft runout.

Instrumentation

Two capacitance probes, which measured the movement of the test vessel during a test, were mounted outside the test vessel on the stationary vessel cover, at 90° from each other. The signal from the probes was fed through displacement meters to an X-Y display on an oscilloscope where the actual pattern of motion of the test vessel could be observed and photographed. The orbital frequency of the test vessel motion was measured by a frequency counter.

The temperature of the water in the test vessel was monitored by a thermocouple that extended into the liquid. Test shaft speed was measured with a magnetic pickup head mounted close to a six-toothed gear on the shaft. The signal from the pickup was displayed on a four-channel frequency counter.

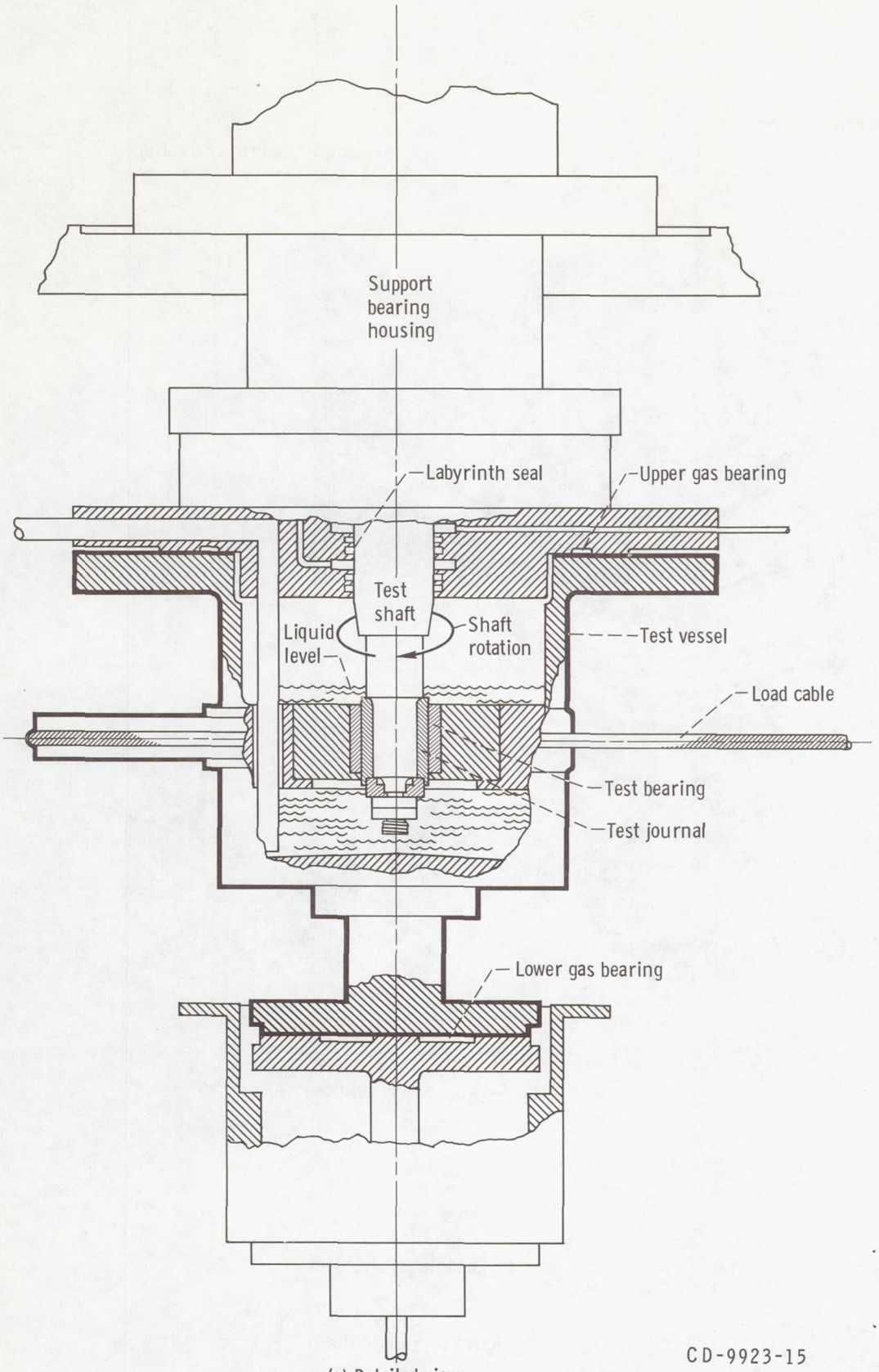

(a) Detailed view.

Figure 3. - Bearing test apparatus.

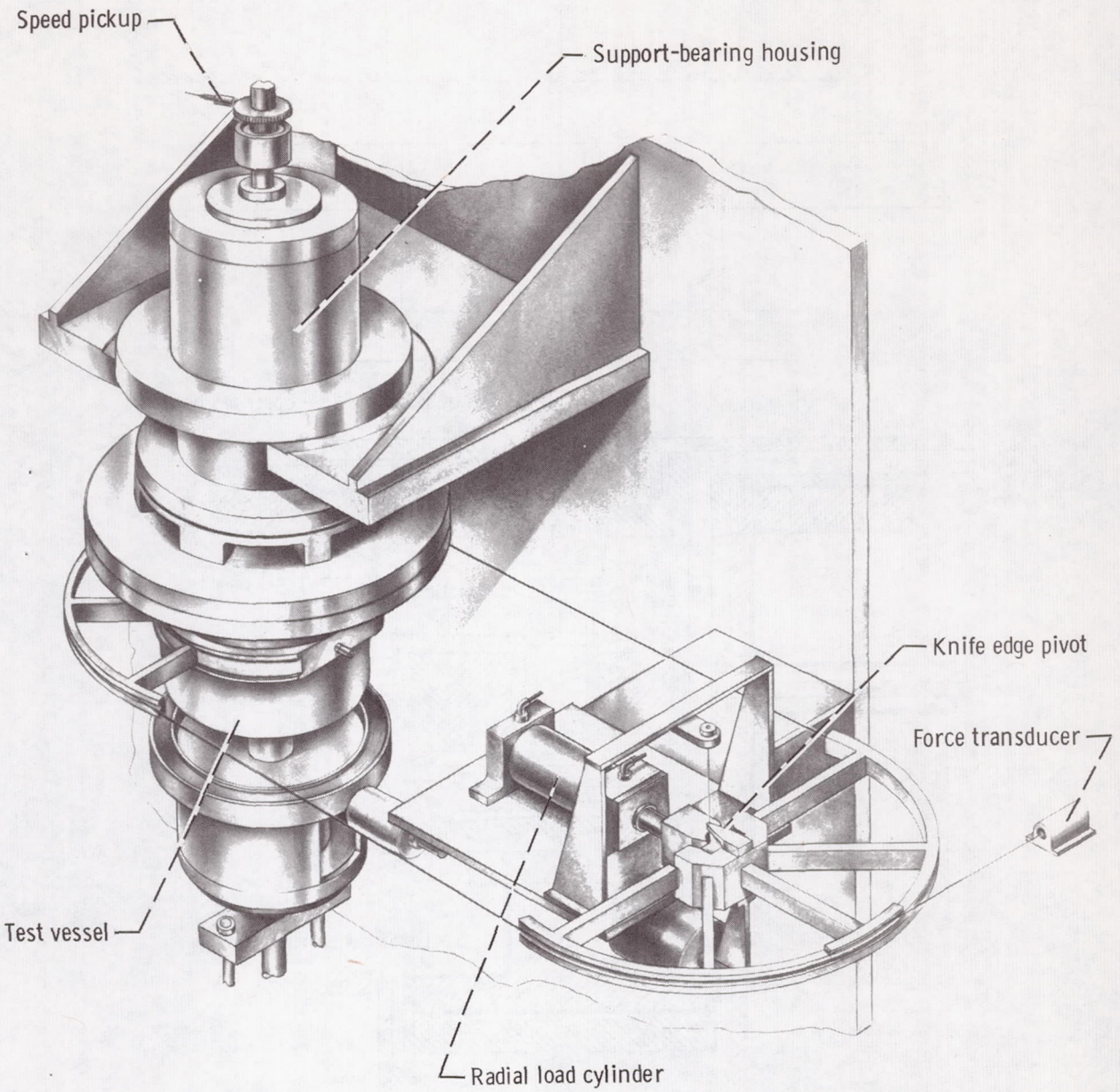

(b) Loading mechanism.

Figure 3. - Concluded.

PROCEDURE

General Pretest Preparation

Prior to each test, the test bearing was assembled into its housing with a slight interference fit. The bearing was then machined in place to the desired inside diameter. Nine bore-gage readings, each accurate to within 0.0001 inch (2.5 μm), were averaged and used as a measure of the bearing diameter. The various diametral clearances were obtained by varying the bearing inside diameter. The outside diameter of the mating journal was ground concentric with its inside diameter within 0.0002 inch (5 μm) to ensure a minimum amount of runout. Because the journals were made of a hard titanium carbide material and the bearings of bronze, the journals did not score or lose any of their original integrity and could be used repeatedly for these tests without remachining their outside diameters.

After the journal was assembled onto the shaft, the vessel containing the test bearing was filled with water and carefully raised into position around the journal by the lower air cylinder.

Test Procedure

The test shaft speed was increased in increments of 1000 rpm from 0 to 12 000 rpm (maximum). Radial load was kept at zero until a speed was reached where fractional frequency whirl occurred. The onset of whirl was noted by observing the bearing motion on the oscilloscope screen. The whirl onset speed was recorded and a load was applied to the bearing to stabilize it before the next higher speed was attempted. At each speed, sufficient load was maintained to keep the test bearing stable. The load was then slowly decreased until the first signs of fractional frequency whirl were apparent. The load and speed were then recorded and photographs of the x-y and time displacement oscilloscope traces of bearing motion were taken before the load was again increased and the next higher speed attempted. This procedure was repeated until the maximum speed of 12 000 rpm was attained. In some cases the bearing motion at the higher speed levels reached such high amplitudes that the maximum speed could not be attained without risking bearing failure. For this reason some tests had to be shortened.

The time interval between speed and load changes varied but was of sufficient duration to allow the friction torque to stabilize. Speed, load, lubricant temperature, and bearing friction torque were recorded at each speed and load condition. Test vessel movement was noted by observation of the oscilloscope screen in order to identify bearing instability at each test interval.

RESULTS AND DISCUSSION

Bearing Instability

The bearing instability of principal concern here is fractional frequency whirl. Figure 4 illustrates simply the origin of this self-excited whirl phenomenon in a full cylindrical bearing. When the shaft is displaced by a load W from a concentric position within the bearing, a pressure buildup occurs in the fluid film. A force component F_w acting at right angles to the eccentricity e is produced and, if great enough, will cause the shaft center to whirl about the bearing center at approximately one-half the speed of the shaft. Application of a larger load to the bearing will decrease its attitude angle, φ, and may reduce the whirl-producing force component F_w to a value too small to sustain the fractional frequency whirl. Thus, application of a larger load may result in stable operation.

Usually, in any bearing stability investigation, the motion of the test shaft is monitored. However, in the experiments reported herein, the motion of the bearing with its massive housing was monitored. In order to establish the validity of the stability data obtained in this investigation, a three-axial groove bearing was run in water with a plain

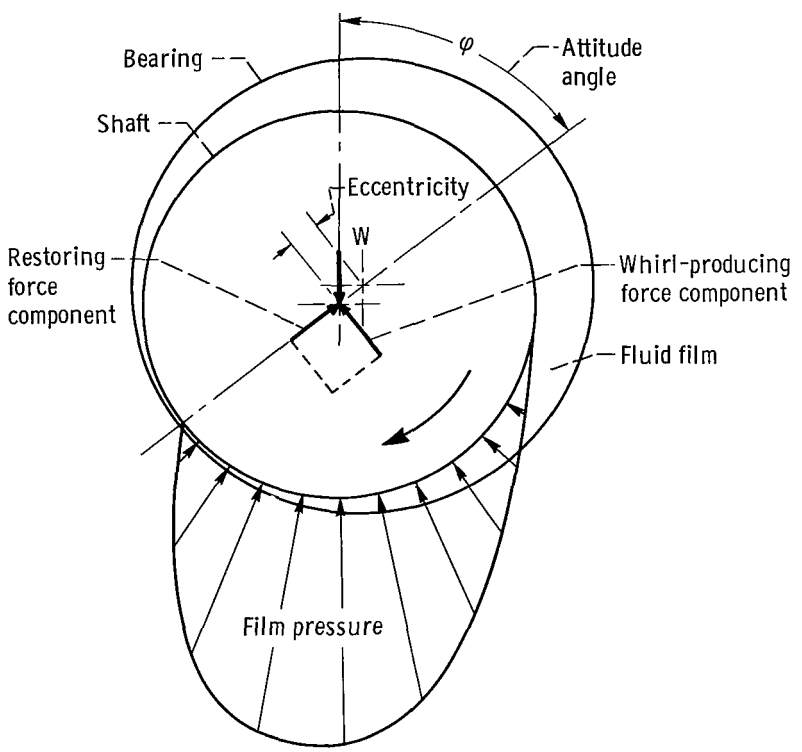

Figure 4. - Self-excited fractional frequency whirl phenomenon.

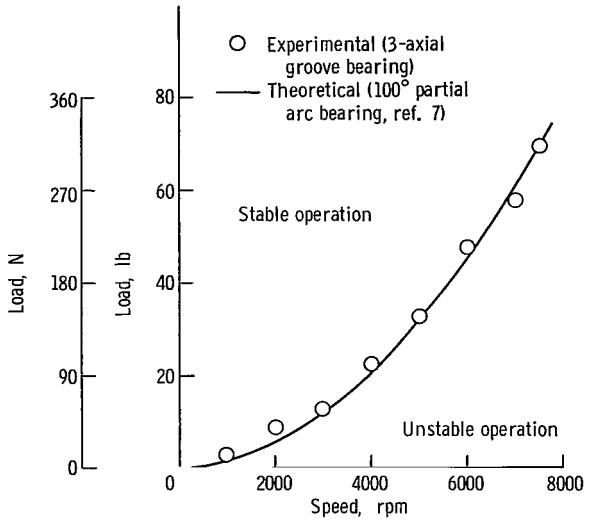

Figure 5. - Comparison of theoretical stability characteristics of 100° partial arc bearing with experimental data for three-axial groove bearing. Length to diameter ratio, 1; radial clearance, 0.0008 inch (20 μm).

journal. The results were compared with the theoretical curve of a 100° partial-arc bearing (ref. 7) as shown in figure 5. (The 100° partial-arc bearing has stability characteristics similar to those of the three-axial groove bearing). Excellent correlation was obtained between theoretical and experimental data, which indicated that the test apparatus and its monitoring system were highly reliable.

Figure 6(a) shows oscilloscope traces of bearing motion with a 20 fully grooved herringbone journal bearing in water with a 15-pound (67-N) load. The load was sufficient to result in stable bearing operation as indicated by the small pattern of bearing motion. When the load was decreased to 3 pounds (13 N), however, fractional frequency whirl ensued. The rather large elliptical whirl pattern observed on the oscilloscope screen is shown in figure 6(b). If the bearing was allowed to operate unstably, the supporting film between the bearing and journal would break down, and the bearing would eventually fail.

When whirl occurs, the journal (or bearing, in this case) operates at a whirl frequency that will allow it to develop a large amplitude excursion (This is a condition of zero pressure buildup in the film under whirl conditions). The film pressure buildup is zero only if the whirl speed matches the pumping speed (average velocity in the film). At zero eccentricity, the average circumferential velocity in the film is one-half the journal surface speed. For stable operation and nonzero eccentricity the average pumping speed is less than one-half the journal surface speed because of the pressure buildup in the film.

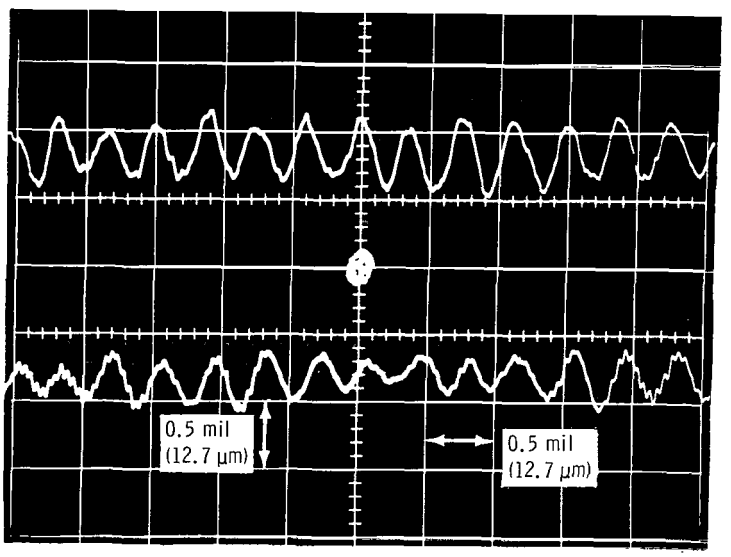

(a) Stable operation at 4000 rpm; load, 15 pounds (67 N).

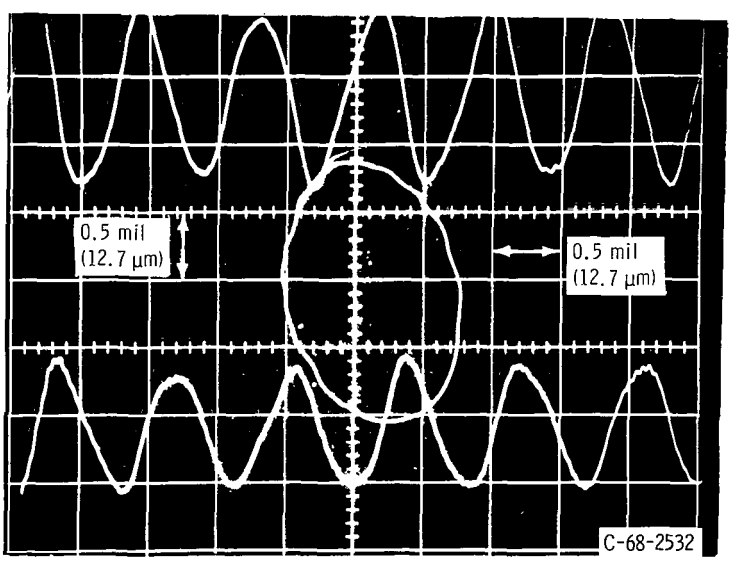

(b) Unstable operation (fractional frequency whirl) at 4000 rpm; load, 3 pounds (13 N).

Figure 6. - X-Y and time traces of bearing motion of 20 fully grooved herringbone journal in water. Bearing B-4 with journal K-6. Radial clearance, 0.0014 inch, (36 μm); time trace, 20 milliseconds per centimeter.

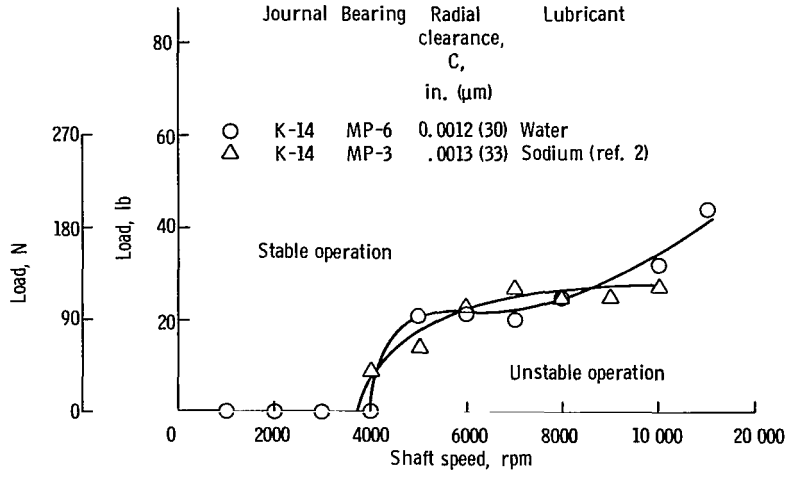

Figure 7. - Comparison of stability of bearing and journal having similar geometric characteristics in sodium at 500° F (533 K) and water at room temperature (300 K).

Good agreement existed between the stability characteristics of herringbone-grooved journal bearings run in water and similar bearings previously run in sodium (ref. 2) as shown in figure 7. The 20 partially grooved herringbone journal K-14 was used in both tests and the radial clearance in the two bearings varied by only 0.0001 inch (3 μm) from each other. The correlation obtained in these tests indicates that water testing can be employed for stability investigations of bearings that eventually would be operating in some of the liquid metals.

Herringbone-Groove Journal Bearings

Experimental results obtained with three journals having different groove geometries are shown in table II and in figures 8 to 13. The bearings were submerged in water at a temperature range from 72° to 89° F (296 to 305 K) (temperature variation was so small as to have negligible effect on the results) and run hydrodynamically over a speed range of 1000 to 12 000 rpm at unit loads from 0 to 36.9 psi (25.5×10^4 N/m^2). Eleven tests were conducted at radial clearances ranging from 0.0003 to 0.0017 inch (8 to 43 μm).

Table III shows the fractional frequency whirl characteristics of bearing B-4 run with a 20 fully grooved herringbone journal K-6. As the shaft speed was increased, the minimum load at which whirl was suppressed also increased, and the whirl ratio decreased. Fractional frequency whirl is often referred to as "half-frequency whirl" but, because the whirl ratios can drop to a value much less than 0.5 (cf. 0.3, table III, also

TABLE II. - TEST RESULTS ON THREE HERRINGBONE GROOVED JOURNALS

Bearing	Journal	Radial clearance, C		Ratio of groove clearance to ridge clearance, H	Number of grooves and groove type	Fractional frequency whirl onset speed at zero load, N_S, rpm	Maximum shaft speed, rpm	Maximum unit load	
		in.	μm					psi	N/m^2
MP-6	K-14	0.0012	30	2.1	20 partial	4 100	11 000	36.9	25.5×10^4
B-14	↓	.0010	25	2.5	↓	5 400	11 000	22.2	15.2
MP-10	↓	.0007	3	3.0	↓	6 100	9 800	21.3	14.5
MP-12	↓	.0003	8	5.7	↓	>12 000	12 000	13.3	9.0
MP-5	K-15	0.0017	43	2.0	40 partial	3 000	12 000	34.2	23.4×10^4
MP-10	↓	.0008	20	3.1	↓	6 100	10 000	35.1	24.1
MP-12	↓	.0005	13	4.4	↓	7 100	8 000	31.1	21.4
B-4	K-6	0.0014	36	2.3	20 full	3 100	12 000	26.7	18.6×10^4
B-2	↓	.0010	25	2.6	↓	7 100	11 000	26.7	18.6
B-3	↓	.0006	15	3.6	↓	6 100	9 000	33.4	23.0
B-5	↓	.0008	20	3.1	↓	6 100	10 000	31.6	21.8

TABLE III. - LOAD AND WHIRL RATIOS AT INCIPIENT WHIRL CONDITIONS FOR VARIOUS SPEEDS

[Bearing B-4 and 20 full-groove herringbone journal K-6.]

Shaft speed, rpm	Minimum load to suppress whirl		Whirl ratio, ω_w/ω
	lb	N	
4000	3	13	0.45
5000	6	27	.42
6000	19	85	.38
7000	28	125	.34
8000	36	160	.31

ref. 6), it appears that the term fractional frequency whirl is more descriptive of the actual phenomenon.

A study of figures 8 to 10 reveals that fractional frequency whirl threshold speeds at zero load are most affected by the radial clearance. Generally, the smaller the radial clearance, the higher the whirl threshold speed at zero load. The one exception was the 20 fully grooved herringbone journal (fig. 10) where the maximum zero load whirl thres-

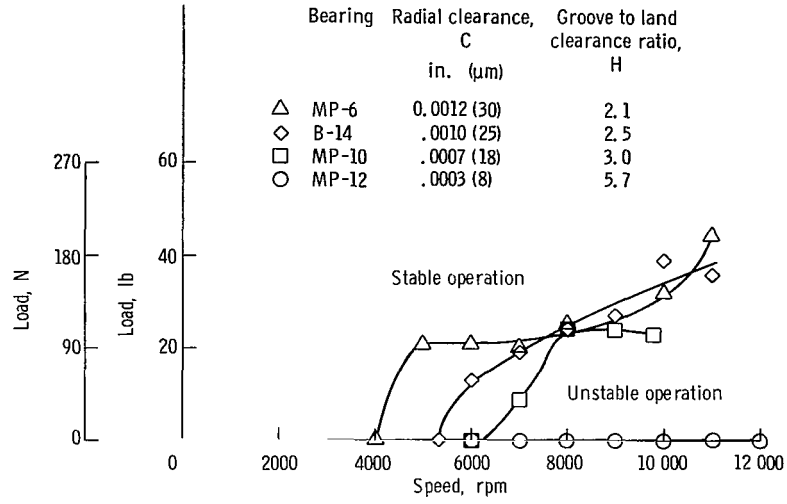

Figure 8. - Stability characteristics of 20 partially grooved herringbone journal K-14 with plain bearing at various radial clearances.

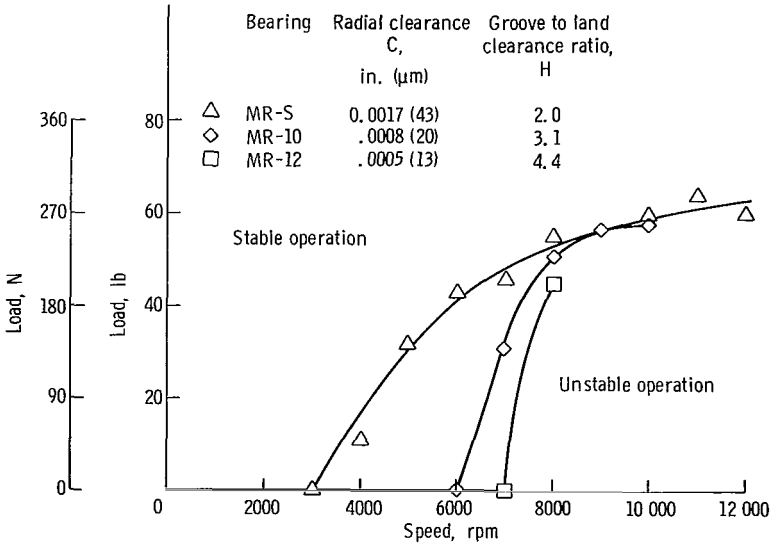

Figure 9. - Stability characteristics of 40 partially grooved herringbone journal K-15 with plain bearing at various radial clearances.

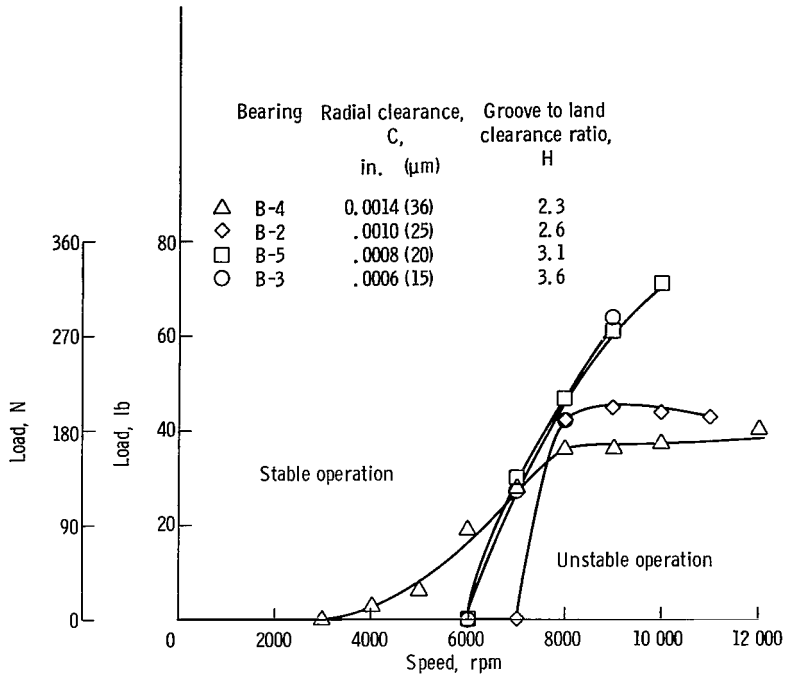

Figure 10. - Stability characteristics of 20 fully grooved herringbone journal K-6 with plain bearing at various radial clearances.

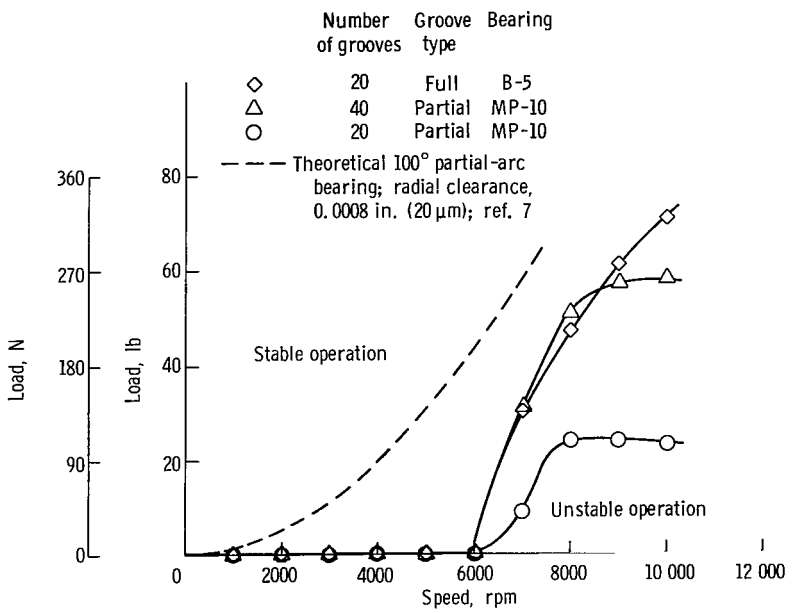

Figure 11. - Effect of groove geometry on stability of herringbone journal bearings. Groove to land clearance ratio, 3.0 to 3.1; bearing radial clearance, 0.0007 to 0.0008 inch (18 to 20 μm).

hold speed of 7100 rpm was obtained with a radial clearance of 0.0010 inch (25 μm) rather than the minimum clearance of 0.0006 inch (15 μm). These results indicate that the fully grooved herringbone journal bearings have somewhat different stability characteristic than the partially grooved.

All three journal configurations, the 20 partial-herringbone groove, the 40 partial-herringbone groove, and the 20 full-herringbone groove, had better stability characteristics than the theoretical 100° partial-arc bearing (fig. 11), especially at zero load. Of the three herringbone journals tested, the 20 partial-groove herringbone journal bearing had the best stability characteristics under load because it required a lesser load at any given speed to keep it stable. This is shown in figure 11 where the three herringbone configurations are compared at essentially the same clearances and groove to land clearance ratios H. At 9000 rpm, for example, the 20 fully grooved and 40 partially grooved journals required approximately 60 pounds for stability, whereas the 20 partially grooved journal remained stable until the load had been reduced to approximately 24 pounds. However, no significant difference in the zero load threshold of stability was observed

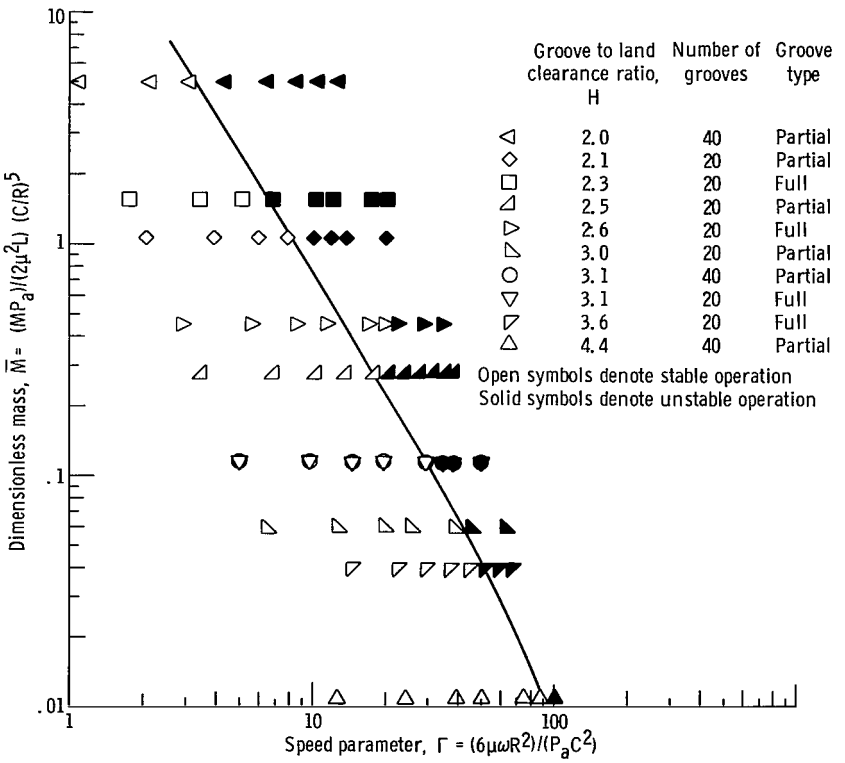

Figure 12. - Experimental stability characteristics for 20 and 40 partially and 20 fully grooved herringbone journals with plain bearings. Groove depth, 0.0014 to 0.0017 inch (36 to 43 μm).

among the three configurations of journals tested. At zero load all three became unstable at shaft speeds immediately above 6000 rpm.

Figure 12 shows a stability plot of dimensionless rotor mass $\overline{M}$ as a function of dimensionless speed parameter Γ for data at various radial clearances for the three herringbone configurations tested. The open symbols indicate conditions of stable operation, and the solid symbols, conditions of fractional frequency whirl. A smooth curve is drawn through the points representing the highest speed attained under stable operation at zero load for each test condition; this separates the stable from the unstable zones of operation. The fact that a smooth curve resulted indicates that the number of grooves, 20 or 40, had no appreciable effect on bearing stability, at least not for journals having groove depths in the range tested (0.0014 to 0.0017 in. (36 to 43 μm)). A discrepancy does exist in the data for the 20 fully grooved journal bearings at $\overline{M}$ values of 1.57 and 0.45 (fig. 12), indicating that a partially and a fully grooved herringbone journal bearing have different stability characteristics at certain radial clearance conditions.

The effect of groove to land clearance ratio H on stability could not be determined in this investigation because the groove depths of the three herringbone configurations were held relatively constant (0.0014 to 0.0017 in. (36 to 43 μm)). The various values of H were obtained by changing the radial clearances, and it is the effect of these radial clearance variations that appears in the recorded data.

Figure 13 shows a comparison of the experimental data of figure 12 with theoretical results obtained for the herringbone-grooved journal bearings of this investigation. The theoretical stability analysis is presented in the appendix. It is represented by the dashed curve to the right of the solid experimental curve in figure 13 and predicts a larger range of stable operation than observed experimentally. Similar results were reported (ref. 3) on experiments with herringbone-groove rotors in air, indicating that there may be an important parameter missing in the theoretical analysis. The analysis assumes (1) an infinite number of grooves in the herringbone configuration, and (2) laminar flow. Actually, the experimental data of this report were obtained from journals having a finite number of herringbone grooves (20 and 40) and the bearings may well have been under the influence of partially or fully turbulent flow conditions.

Bearing MP-12 mated with journal K-14 had a radial clearance of 0.0003 inch (8 μm) (table II). The groove depth of journal K-14 was 0.0014 inch (36 μm) (table I). The groove radial clearance of this bearing combination is the sum of the radial clearance and the groove depth, or 0.0017 inch (43 μm). From figure 14 (see p. 20), for example, for a plain bearing and journal at a radial clearance of 0.0017 inch (43 μm) and at a water temperature of 80° F (300 K), turbulent flow conditions can be expected at shaft speeds above approximately 9000 rpm. Therefore, turbulent conditions could have existed in the groove areas of this herringbone-groove journal-bearing combination at the higher speeds. This was at the minimum radial clearance condition of all the experimental tests.

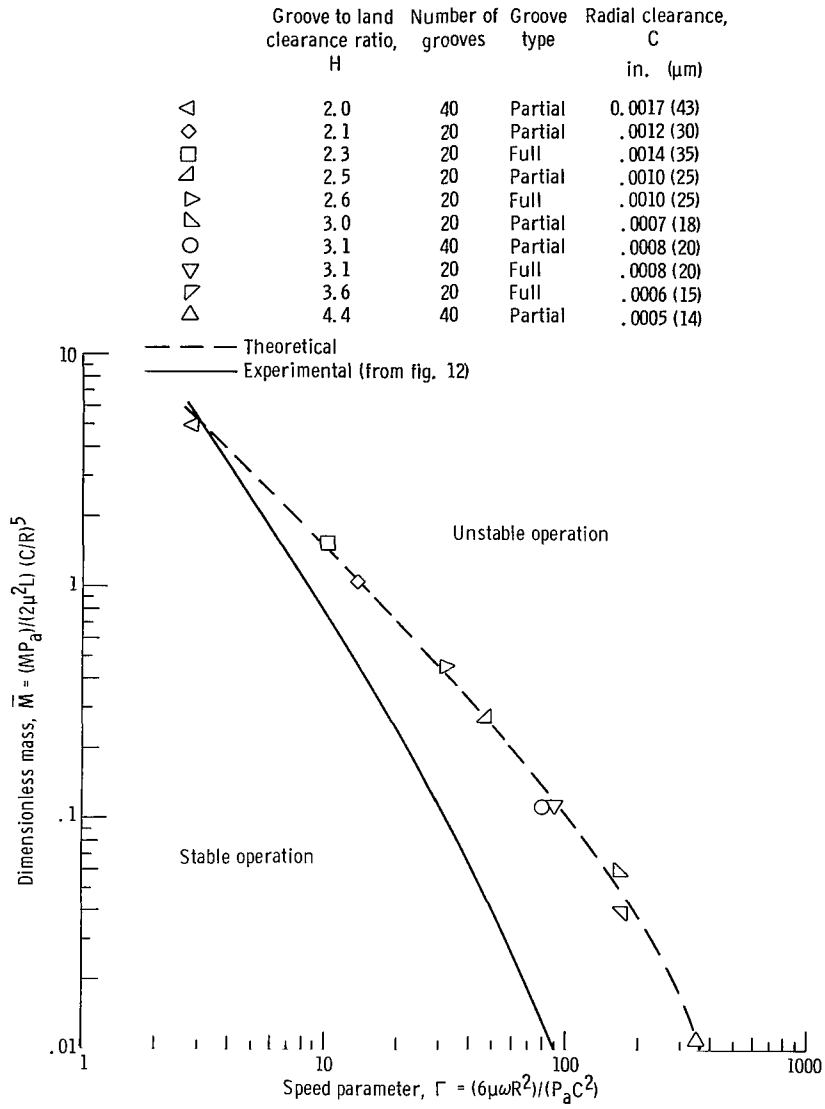

Figure 13. - Comparison of experimental with theoretical stability data for 20 and 40 partially and 20 fully grooved herringbone journals with plain bearings.

At the maximum clearance condition (bearing MP-5 and journal K-15 (table II)), the radial clearance was 0.0017 inch (43 μm), and the groove depth was 0.0017 inch (43 μm) (table I), which results in a groove radial clearance of 0.0034 inch (86 μm). Under these conditions, assuming a plain bearing and journal having this clearance, turbulent flow in the grooves could be expected at shaft speeds above 3100 rpm (fig. 14). Hence, it is concluded that some turbulent flow existed in the test bearings during this investigation that could have influenced the experimental results.

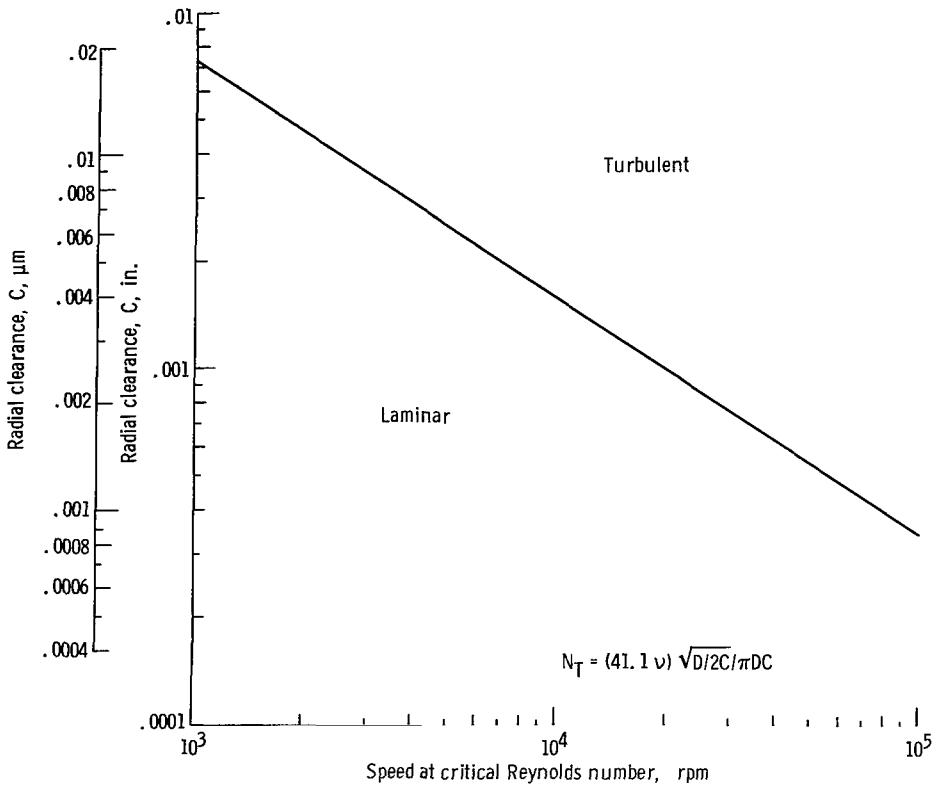

Figure 14. - Theoretical radial clearance versus speed at critical Reynolds number for 1.5-inch (3.8-cm) diameter plain journal bearing in water at 80° (300 K).

The analysis of turbulent flow for a herringbone journal is difficult to perform because the transition from laminar to turbulent flow depends not only on surface roughness but also on the centrifugal forces and pressure forces generated in the bearing (refs. 8 and 9). The analysis has been simplified by assuming that the groove clearance in the herringbone bearing can be compared with the radial clearance of a plain bearing in determining whether laminar or turbulent conditions existed. The accuracy of this assumption could be determined by running a series of herringbone journal-bearing tests in a liquid having a viscosity great enough to ensure laminar flow conditions throughout the selected test range. These experimental data could then be compared with the theoretical analysis which is based on laminar flow conditions.

SUMMARY OF RESULTS

A series of hydrodynamic journal bearing stability tests was run in water at an average temperature of 80° F (300 K) at speeds to 12 000 rpm and radial loads from zero to 36.9 psi (25.5×10^4 N/m^2). Plain bearings were run at various clearances with a partially

grooved herringbone journal having 20 groove-ridge pairs, a fully grooved herringbone journal having 20 groove-ridge pairs, and a partially grooved herringbone journal having 40 groove-ridge pairs. The bearing diameter in all cases was nominally 1.5 inches (3.8 cm) and the bearing had a length-to-diameter ratio of 1. The following results were obtained:

1. The stability of herringbone journal bearings was far superior to that of a 100^{o} partial-arc bearing, especially at zero load.

2. The 20 partially grooved herringbone journal bearing required lower loads to maintain stability than did the 20 fully grooved or 40-partially grooved journal bearings. However, no significant differences in the zero load threshold of stability were observed among the three configurations at the 0.0014- to 0.0017-inch (36- to 43-μm) groove depths tested.

3. Experimental data on stability of herringbone groove bearings did not correlate well with the theoretical laminar flow analysis. Theoretical analysis predicts a larger range of stable operation than was observed experimentally.

4. Good agreement existed between the stability characteristics of herringbone grooved journal bearings run in water and similar bearings previously run in sodium.

5. Fractional frequency whirl ratio (ω_w/ω) decreased as the load required for stability increased.

6. Fractional frequency whirl threshold speeds are most affected by the radial clearance. Generally, the smaller the radial clearance, the higher the fractional frequency whirl threshold speed.

7. Experimental stability data for a three axial grooved bearing showed excellent agreement with the theory for a 100^{o} partial-arc bearing.

Lewis Research Center,
National Aeronautics and Space Administration,
Cleveland, Ohio, July 16, 1968,
120-27-04-03-22.

APPENDIX - STABILITY ANALYSIS FOR INCOMPRESSIBLY LUBRICATED HERRINGBONE-GROOVE JOURNAL BEARINGS

The stability limit for an unloaded journal bearing can be determined from a knowledge of the small amplitude steady whirling characteristics of the bearing (ref. 10). For gas lubricated herringbone-groove journal bearings, an analysis of small amplitude whirling is presented in reference 5. This analysis assumes laminar flow conditions in the bearing. Furthermore, it is assumed that the eccentricity remains small enough so that the pressure in the fluid film is adequately represented by

$$P(x,\theta^*) = P_0(x) + \epsilon P_1(x,\theta^*) \tag{1}$$

For an incompressible lubricant, several terms of the differential equation derived in reference 5 disappear. What remains is

$$\frac{C_1}{P_a}\frac{\partial^2 P_1}{\partial x^2} + \frac{C_3}{P_a}\frac{\partial^2 P_1}{\partial x\,\partial\theta^*} + \frac{C_5}{P_a}\frac{\partial^2 P_1}{\partial\theta^{*2}} + C_6 \sin\theta^* = 0 \tag{2}$$

wherein the coefficients C_1, C_3, C_5, and C_6 are functions of α, β, H, ω_w, Γ, L/D, and P_0 and are given in reference 5. The concentric pressure distribution P_0 appears as a factor in each of these coefficients; consequently, the analysis may be simplified by dividing equation (2) by P_0. When either the grooved or the smooth member of the bearing is stationary, the speed parameter Γ (Λ in ref. 5) may be factored from the coefficient C_6. Moreover, Γ does not appear in C_1, C_3, or C_5. Thus, if P_1/Γ is taken as a new dependent variable in equation (2), one solution may be obtained that is valid for all values of Γ. The steady whirl solution may now be carried through as in reference 5.

According to the analysis of reference 10, the stability limit may be determined from the steady whirl solution. The procedure is as follows: The whirl ratio ω_w/ω is varied until the tangential force F_w is zero. The radial force F_r is then equal to the centrifugal force due to a critical mass M_c whirling with frequency ω_w in a circle of radius e.

$$F_r = M_c e \omega_w^2 \tag{3}$$

The dimensionless critical mass parameter $\overline{M}_c$ is then given by

$$\overline{M}_c \equiv \frac{M_c P_a}{2\mu^2 L}\left(\frac{C}{R}\right)^5 = \frac{36F_r}{\Gamma^2 \epsilon P_a LD}\left(\frac{\omega}{\omega_w}\right)^2 \tag{4}$$

In reference 10 it is shown that $\overline{M}_c$ is an upper limit of $\overline{M}$ for stability if $\partial F_w/\partial\omega_w$ is negative. For the incompressibly lubricated herringbone bearing this proved to be the case for all the geometries studied.

A FORTRAN IV computer program has been written to carry out this analysis. Input to the program consists of the helix angle β, groove width ratio α, groove depth ratio H, bearing length to diameter ratio L/D, the proportion of the bearing length that is grooved L_1/L, and whether the smooth or grooved member of the bearing is rotating. Sample input data are appended to the FORTRAN program listing which follows this text. Two data lines are shown, but any number may be used. The first indicates that $\beta = 33^o$, $\alpha = 0.5$, H = 2.5, L/D = 1.0, and $L_1/D = 0.6667$. The final -1 indicates that the grooved member of the bearing is rotating; if the smooth member were rotating, +1 would be shown. The parameters on the second data line are the same except that H = 2.1 and $L_1/L = 1$.

Table IV shows the output obtained for the two input lines just described. For each case, the input data are printed, followed by certain coefficients appearing in the differential equation (2). There follows a table of various quantities dependent on the whirl ratio ω_w/ω. These are the dimensionless bearing load, in the forms $W/\Gamma\epsilon P_a LD$ and ϵS, the attitude angle φ, dimensionless critical masses in the forms

TABLE IV. - HERRINGBONE BEARING VOHR AND CHOW ANALYSIS STABILITY CALCULATIONS

[Incompressible lubricant; grooved member rotating; helix angle, 33^o; groove width ratio, 0.5; length to diameter ratio, 1.0.]

(a) Groove to land clearance ratio, 2.5; groove length to bearing length ratio, 0.6667. Constants: C_3, -3.1029; C_5, 6.7630; C_{6A}, 0.1609; C_{6B}, 1.0560; CP, 0.1591

Whirl ratio, ω_w/ω	Bearing load		Attitude angle, φ	Stability parameters		Radial load, $F_r/\Gamma\epsilon P_a LD$	Tangential load, $F_w/\Gamma\epsilon P_a LD$	Runge Kutta ΔX	Constant, C_6
	$W/\Gamma\epsilon P_a LD$	ϵS		$eM_c\omega/\mu L(C/R)^3$	$\overline{M}_{cr}\sqrt{S}$				
0	0.1517	0.1749	53.292	0	0	0.09068	0.1216	0.04167	1.2169
.5000	.09068	.2925	.4936	13.058	.5885	.09068	$.7812\times10^{-3}$	.04167	.1609
.6000	.09365	.2833	-14.462	9.0679	.4904	.09068	$-.2339\times10^{-1}$	.04167	-.05027
.5032	.09068	.2925	0.1733×10^{-6}	12.891	.5848	.09068	$.2743\times10^{-9}$	.04167	.1541

(b) Groove to land clearance ratio, 2.1; groove length to bearing length ratio, 1.0. Constants: C_3, -2.1765; C_{6A}, 0.07651; C_{6B}, 1.4329; CP, 0.1449

0	0.1484	0.1787	51.390	0	0	0.09263	0.1160	0.06205	1.5094
.5000	.09312	.2849	-5.9183	13.338	.5948	.09263	$.9602\times10^{-2}$	.06250	.07651
.4000	.09392	.2824	9.5097	20.841	.7435	.09263	$.1552\times10^{-1}$	.06250	.3631
.4618	.09263	.2864	$.1387\times10^{-5}$	15.638	.6441	.09263	$.2242\times10^{-8}$	.06250	.1861

$3M_c\omega(C/R)^3/\mu L \equiv \overline{M}_c\Gamma$ and $\overline{M}_{cr}\sqrt{S}$ (where M_{cr} is the dimensionless mass used in ref. 2), dimensionless radial and tangential forces $F_r/\Gamma\epsilon P_a LD$ and $F_w/\Gamma\epsilon P_a LD$, the step size in the Runge-Kutta integration, and the coefficient C_6. The first line, for a whirl ratio of zero, is the steady-state solution. The whirl ratio is then varied until F_w is within a prescribed bound of zero. This condition is shown in the last line of the table, and it is the stability parameters appearing in this line that represent the critical mass derived in the preceding analysis.

The program listing follows.

```
$IBFTC INCOM
      COMMON /CBON/ C6A,C6B,L,L1,DN
      COMMON /COMD/ C3,C5,C6
      COMMON /CVR/ CDO, CD2, DQL
      REAL L,L1,LS
      COMPLEX CDO
      EPSF = 1.E-4
      WRITE (6,699)
699   FORMAT (1H2)
4     READ(5,5) BETA, ALFA, H, L, L1, SGN
5     FORMAT (6F8.0)
C  BETA=HELIX ANGLE,DEG.  ALFA=GROOVE WIDTH/TOTAL WIDTH RATIO.  H=GROOVE
C  CLEARANCE/LAND CLEARANCE.  L=LENGTH/DIAMETER.  L1=GROOVED LENGTH/TOTAL
C  LENGTH.  SGN=+1.0 FOR SMOOTH MEMBER ROTATING, -1.0 FOR GROOVED MEMBER
C  ROTATING.
      IF (L.EQ.0.) STOP
      WRITE (6,7)
7     FORMAT (1H2/20X, 71HHERRINGBONE BEARING - INCOMPRESSIBLE LUBRICANT
     1 - VOHR AND CHOW ANALYSIS // 20X, 22HSTABILITY CALCULATIONS )
      IF (SGN.LT.0.) GO TO 9
      WRITE (6,801)
801   FORMAT (1H+ 60X,  22HSMOOTH MEMBER ROTATING )
      GO TO 902
9     WRITE (6,901)
901   FORMAT (1H+ 60X, 23HGROOVED MEMBER ROTATING )
902   WRITE(6,6) BETA, ALFA, H, L, L1
6     FORMAT (6HL BETA 10X,4HALFA 12X,1HH 12X,3HL/D 10X,4HL1/L /5G14.4)
      BETA= BETA/57.2957796*SGN
      SI= SIN(BETA)
      CO= COS(BETA)
      ALFI= 1.-ALFA
      H2= H*H
      H3= H2*H
      DN= ALFA+ALFI*H3
      L= 2.*L
      LS = SGN*L
      H32= (H3-1.)**2
      AA= ALFA*ALFI
      AS= AA*SI*SI
      ASC= AA*SI*CO
      D2= H3+AS*H32
      H31= (H3-1.)*(H-1.)
      C1= D2/(DN*L)
      C3 = 2.*ASC*H32*L/D2
      C5= (H3 + AA*CO*CO*H32)*L/(DN*C1)
      C6A = -3.*AS*(H-1.)**2*LS/(DN*DN)*(AA*H32*CO*CO*(ALFI*H2*(H2+H-1.)
     1 -ALFA*(H2-H-1.))/D2 - H2)/C1
      C6B = L/C1
      CP = ASC*H31*LS/D2
      WRITE (6,10) C3,C5, C6A, C6B, CP
10    FORMAT (3HKC3 G12.4, 4H  C5 G12.4, 5H  C6A G12.4, 5H  C6B G12.4,
     1 4H  CP G12.4)
      WRITE (6,15)
15    FORMAT ( 46HLWHIRL RATIO  BRG LOAD   SOMMERFELD  ATT ANGLE 4X,
     1 20HSTABILITY PARAMETERS 4X, 8HRAD LOAD 4X,22HTAN LOAD   RUNGE KUT
     2TA /11H W3/(W1+W2)4X,7HW/AEPLD 5X,6HNR*EPS 7X,3HPHI 5X,34H3MWC3/LM
```

```
     3UR3    MCR*S**.5    FR/AEPLD 4X,8HFT/AEPLD 7X,2HDX 10X,2HC6 )
      CD2 = AS*H32 + H3
      CDQ = (0.,1.)*ASC*H32*L
      DQL = 3.*((H3 + AS*H31*(H2+H-1.)/H)*CP + ASC*LS*(H-1.)**2/H)
      CALL BONE (0.,FT0)
      W1 = .5
      CALL BONE (W1,FT1)
      SG1 = SIGN(.1,FT1)
      W2 = W1
      DO 215 J = 1, 15
      W2 = W2 + SG1
      CALL BONE (W2,FT2)
      SG2 = SIGN(.1,FT2)
      IF (SG2 - SG1) 220, 210, 220
210   W1 = W2
215   FT1 = FT2
      GO TO 4
220   DO 235 J = 1, 10
      W = (FT2*W1 - FT1*W2)/(FT2-FT1)
      CALL BONE (W,FT)
      IF(ABS(FT/FT0).LE.EPSF) GO TO 4
      IF(ABS(FT2).GT.ABS(FT1)) GO TO 230
      FT1 = FT2
      W1 = W2
230   FT2 = FT
235   W2 = W
      GO TO 4
      END

$IBFTC BONES
      SUBROUTINE BONE (W3,FT)
      COMMON /CBON/ C6A,C6B,L,L1,DN
      COMMON /CBR/ XF, JK, KS, KC, Y
      COMMON /COMD/ C3,C5,C6
      COMPLEX JK,KS,KE,KC,TDX,XF,DX,Y(4),A(2),B(2),Q,QI
      REAL L,L1
      XF = .5*L1
      WR = 1. - 2.*W3
      C6 = C6A + WR*C6B
      DX = .0625*L1
      TX = REAL(DX)
      IF (L1.EQ.1.) GO TO 20
      JK = -(0.,1.)*WR
      KE = EXP(L*(XF-.5))
      KC = 1./KE
      KS = .5*(KE - KC)
      KC = .5*(KE + KC)
      KE = KS/(KC*L)
      KS = L*KS*DN
20    B(1) = (0.,0.)
      B(2) = (1.,-1.)
      CALL RKCN (B(1),DX,A(1))
      Q = Y(2)
      QI = Y(4)
      CALL RKCN (B(2),DX,A(2))
      Y(2) = (A(2)*Q  - A(1)*Y(2))/(A(2)-A(1))
      Y(4) = (A(2)*QI - A(1)*Y(4))/(A(2)-A(1))
      IF (L1.EQ.1.) GO TO 125
      Y(4) = Y(4) - JK*(XF-.5) - KE*(Y(2)-JK)
125   Y(4) = -Y(4)*3.14159265
```

```
      FR = REAL(Y(4))
      FT = AIMAG(Y(4))
      W= CABS(Y(4))
      PHI = ATAN2(FT,FR)
      SO = 1./(12.*3.14159265*W)
      CMS = 0.
      CMC = 0.
      IF (W3.EQ.0.) GO TO 75
      CMC = 36.*FR/W3**2
      CMS = 1./(2.*3.14159265)*SQRT(COS(PHI)/SO)/W3
75    PHI = 57.2957796*PHI
      WRITE (6,76) W3,W,SO,PHI,CMC,CMS,FR,FT,TX,C6
76    FORMAT (/10G12.4)
      RETURN
      END

$IBFTC RKCNT
      SUBROUTINE RKCN (YIN,DX,A)
      COMMON /CVR/ CDO, CD2, DQL
      COMMON /CBR/ XF, JK, KS, KC, Y
      COMPLEX CDO,Y(4),AT(4),BT(4),YIN,A,DX,XF,JK,KS,KC
      EXTERNAL DIRGE
      Y(1)= 0.
      Y(2)= 0.
      Y(3)= YIN
      Y(4)= 0.
      CALL RKGC(DIRGE, Y, XF, DX, AT, BT, 4)
      A = DQL + CDO*Y(2) + CD2*Y(3)
      IF (REAL(XF).GE..5) RETURN
      A = A/KS - (Y(2) - JK)/KC
      RETURN
      END

$IBFTC DIR
      SUBROUTINE DIRGE (Y,YP)
      COMMON /COND/ C3,C5,C6
      COMPLEX Y(4),YP(4)
      YP(1)= 1.
      YP(2)= Y(3)
      YP(3) = C5*Y(2) + (0.,1.)*(C6 - C3*Y(3))
      YP(4)= Y(2)
      RETURN
      END

$IBFTC RKGHC
      SUBROUTINE RKGC (DERIV, Y, XFINAL, DELTA, Q, YP, N)
C  RUNGE-KUTTA-GILL INTEGRATION OF N-1 COMPLEX FUNCTIONS OF COMPLEX
C  ARGUMENT Y(1) FROM Y(1)INITIAL TO XFINAL
      DIMENSION A(4), B(4), C(4)
      COMPLEX Y(1), Q(1), YP(1), XFINAL, DELTA, T
      DATA A/.5, .292893219, 1.70710678, .166666667/, B/2., 1., 1., 2./,
     1     C/.5, .292893219, 1.70710678, .5/
      KK = CABS((XFINAL-Y(1))/DELTA) + .01
      IF (KK.LE.0) GO TO 20
      DO 5 I = 1, N
5     Q(I)=0.
      DO 10 K = 1, KK
      DO 10 J = 1, 4
      CALL DERIV(Y,YP)
      DO 10 I=1,N
      T=A(J)*(YP(I)-B(J)*Q(I))
      Y(I)=Y(I)+DELTA*T
10    Q(I)=Q(I)+3.*T-C(J)*YP(I)
20    RETURN
      END

$DATA
33.      .5       2.5      1.       .6667    -1.
33.      .5       2.1      1.       1.       -1.
```

REFERENCES

1. Slone, Henry O.; and Lieblein, Seymour: Electric Power Generation Systems for Use in Space. Advances in Aeronautical Sciences. Vol. 4. Th. von Karman and H. L. Dryden, eds., Pergamon Press, 1962, pp. 1131-1152.

2. Schuller, Fredrick T.; Anderson, William J.; and Nemeth, Zolton: Operation of Hydrodynamic Journal Bearings in Sodium at Temperatures to 800° F and Speeds to 12 000 rpm. NASA TN D-3928, 1967.

3. Cunningham, Robert E.; Fleming, David P.; and Anderson, William J.: Experiments on the Stability of Herringbone-Grooved Gas-Lubricated Journal Bearings to High Compressibility Numbers. NASA TN D-4440, 1968.

4. Malanoski, S. B.: Experiments on an Ultrastable Gas Journal Bearing. J. Lubr. Tech., vol. 89, no. 4, Oct. 1967, pp. 433-438.

5. Vohr, J. H.; and Chow, C. Y.: Characteristics of Herringbone-Grooved, Gas-Lubricated Journal Bearings. J. Basic Eng., vol. 87, no. 3, Sept. 1965, pp. 568-578.

6. Anon.: Design of Gas Bearings. Vol. I: Design notes. Mechanical Technology, Inc., 1966, Figure 6.1.22.

7. Lund, J. W., ed.: Design Handbook for Fluid Film Type Bearings. Part III of Rotor-Bearing Dynamics Design Technology. Rep. MTI-65TR14 (AFAPL TR-65-Pt. III, DDC No. Ad-466392), Mechanical Technology, Inc. May 1965.

8. Muijderman, E. A.: Sprial Groove Bearings. Philips Technical Library, Springer-Verlag, 1966.

9. Burton, R. A.; and Hsu, Y. C.: Fundamental Investigation of Liquid-Metal Lubricated Journal Bearings. Rep. SWRI-1228P8-33, RS-502, Southwest Research Inst., June 20, 1967.

10. Pan, C. H. T.: Spectral Analysis of Gas Bearing Systems for Stability Studies. Rep. MTI-64TR58, Mechanical Technology, Inc., Dec. 15, 1964. (Available from DDC as AD-610870).

NATIONAL AERONAUTICS AND SPACE ADMINISTRATION
WASHINGTON, D. C. 20546

OFFICIAL BUSINESS

FIRST CLASS MAIL

POSTAGE AND FEES PAID
NATIONAL AERONAUTICS AND
SPACE ADMINISTRATION

POSTMASTER: If Undeliverable (Section 158 Postal Manual) Do Not Return

"The aeronautical and space activities of the United States shall be conducted so as to contribute . . . to the expansion of human knowledge of phenomena in the atmosphere and space. The Administration shall provide for the widest practicable and appropriate dissemination of information concerning its activities and the results thereof."

—NATIONAL AERONAUTICS AND SPACE ACT OF 1958

NASA SCIENTIFIC AND TECHNICAL PUBLICATIONS

TECHNICAL REPORTS: Scientific and technical information considered important, complete, and a lasting contribution to existing knowledge.

TECHNICAL NOTES: Information less broad in scope but nevertheless of importance as a contribution to existing knowledge.

TECHNICAL MEMORANDUMS: Information receiving limited distribution because of preliminary data, security classification, or other reasons.

CONTRACTOR REPORTS: Scientific and technical information generated under a NASA contract or grant and considered an important contribution to existing knowledge.

TECHNICAL TRANSLATIONS: Information published in a foreign language considered to merit NASA distribution in English.

SPECIAL PUBLICATIONS: Information derived from or of value to NASA activities. Publications include conference proceedings, monographs, data compilations, handbooks, sourcebooks, and special bibliographies.

TECHNOLOGY UTILIZATION PUBLICATIONS: Information on technology used by NASA that may be of particular interest in commercial and other non-aerospace applications. Publications include Tech Briefs, Technology Utilization Reports and Notes, and Technology Surveys.

Details on the availability of these publications may be obtained from:

SCIENTIFIC AND TECHNICAL INFORMATION DIVISION

NATIONAL AERONAUTICS AND SPACE ADMINISTRATION

Washington, D.C. 20546